ACS APPLIED MATERIALS & INTERFACES

Research Article

www.acsami.org

Vitamin B_1 Derived Blue and Green Fluorescent Carbon Nanoparticles for Cell-Imaging Application

Susanta Kumar Bhunia, Nibedita Pradhan, and Nikhil R. Jana*

Centre for Advanced Materials, Indian Association for the Cultivation of Science, Kolkata 700032, India

Supporting Information

ABSTRACT: A carbon-based fluorescent nanoparticle is considered to be a new generation nontoxic nanoprobe suitable for various bioimaging and sensing applications. However, the synthesis of such a high-quality nanoparticle is challenging, and its application potential is mostly unexplored. Here we report a vitamin B_1 carbonization-based approach for blue and green fluorescent carbon nanoparticles of <10 nm size with a fluorescence quantum of up to 76%. We found that carbonization of vitamin B_1 in the presence of phosphate salt at ~90−130 °C for about 2 h produces highly fluorescent carbon nanoparticles of 1−6 nm size. The particle size and fluorescence property can be controlled by varying the reaction temperature and nature of phosphate salt. Elemental analysis shows the incorporation of a large percentage (up to 48 wt %) of other elements (such as nitrogen, oxygen, phophorus, and sulfur) in the carbon matrix. The chemical structure of vitamin B_1 (thiamine) is unique in a sense that it consists of a large number of heteroatoms along with unsaturated bonds and offers low-temperature carbonization with the formation of a nanoparticle having an optimum ratio of sp^2 and sp^3 carbon atoms. These carbon nanoparticles have high colloidal stability and stable fluorescence and have been used as fluorescent imaging probes.

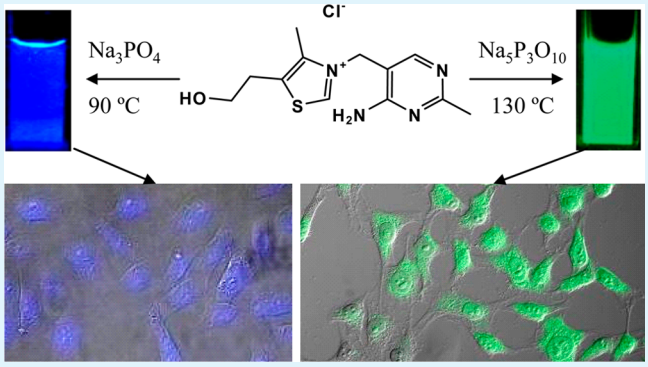

KEYWORDS: *nanoparticle, vitamin, carbonization, fluorescent probe, imaging*

INTRODUCTION

A fluorescent carbon nanoparticle (FCN) is considered to be a new class of nanoparticle suitable for various bioimaging applications.[1] FCNs have been synthesized with tunable visible emission, show high photostability and low toxicity, and are used as potential bioimaging probes.[1−3] Compared to conventionally used fluorescent semiconductor nanoparticles or quantum dots (QDs), which are mainly composed of toxic heavy metals,[4−7] a FCN is made of nontoxic carbon and is expected to be environmentally friendly and biocompatible. However, FCN-based research is relatively less explored compared to other carbon-based nanomaterials like carbon nanotube,[8] fullerene,[9] and graphene.[10] Recently, a new class of molecules having aggregation-induced emission properties have been explored as promising cellular imaging nanoprobes and continue to be an emerging area of development.[11−19] In addition, other nontoxic fluorescent nanoprobes based on silicon nanoparticle,[20] gold cluster,[21] and doped semiconductor nanoparticle[22] are under development.

Different synthetic methods have been explored for FCNs that include electrochemical degradation of graphite rod,[23] laser ablation of a graphite powder,[24] nitric acid oxidation of carbon soot,[25] pyrolysis of carbohydrate[26−29] and ethylenediaminetetraacetic acid salt,[30] thermal degradation of a resol polymer,[31] microwave irradiation of glycerol[32] and amino acid,[33] and microwave-thermal degradation of a glucose−amino acid polymer.[34] The fluorescence quantum yield (QY) is reported to be as high as 69%,[34] although it depends on the synthetic method and emission color.[1] Correlation of the chemical composition with the fluorescence property of FCN shows that the presence of other element such as nitrogen and oxygen has a significant effect on the emission property.[29,34,35] Thus, nitrogen- or oxygen-reach monomer/polymer precursors have been selected so that product FCN can be enriched with those elements.[29,34] Moreover, the synthetic conditions should be finely adjusted to control the particle size typically in the range of 1−10 nm to obtain visible emission. It is expected that the presence of such heteroatoms in a carbon matrix of 1−10 nm size can control the ratio of sp^2 and sp^3 carbon atoms and optimize the lengths of the conjugated double bonds.[29]

Here we show that vitamin B_1 or thiamine can be an ideal precursor material for the synthesis of blue- and green-emitting FCNs via a simple colloid−chemical carbonization approach. The synthesis involves simple heating of vitamin B_1 in the presence of phosphate salt, and the emission of FCN can be tuned by varying the reaction temperature and nature of phosphate salt (Scheme 1). The chemical structure of vitamin B_1 is unique because it consists of a large number of

Received: February 15, 2014
Accepted: April 3, 2014
Published: April 3, 2014

   dx.doi.org/10.1021/am500964d | ACS Appl. Mater. Interfaces 2014, 6, 7672−7679

Scheme 1. Synthetic Strategy for the Preparation of FCNs

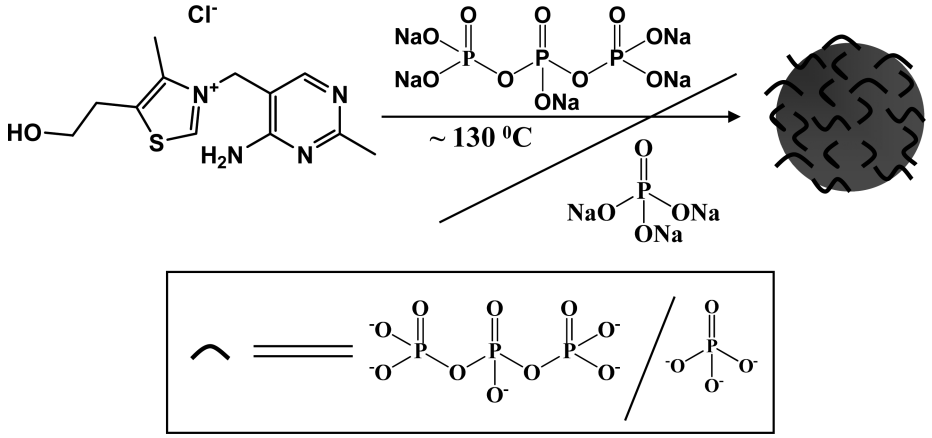

Table 1. Reaction Conditions and Optical Property of Best-Quality FCN Synthesized from Vitamin B_1

capping ligand	wt ratio of vitamin B_1 to ligand	reaction medium	reaction temperature (time)	emission$_{max}$ (excitation)	mol wt/particle size	QY
sodium tripolyphosphate	1:10	water	90 °C (2 h)	430 nm (368 nm)	<2000 Da	~50%
sodium tripolyphosphate	1:1	water	90 °C (2 h)	415 nm (354 nm)	<2000 Da	~42%
sodium tripolyphosphate	10:1	water	90 °C (2 h)	420 nm (400 nm)	<2000 Da	~35%
trisodium phosphate	10:1	water	90 °C (2 h)	440 nm (390 nm)	<2000 Da	~76%
trisodium phosphate	10:1	ethylene glycol	130 °C (2 h)	450 nm (375 nm)	~3.7 ± 0.8 nm	~8%
sodium tripolyphosphate	10:1	ethylene glycol	130 °C (2 h)	470 nm (400 nm)	~5.9 ± 1.8 nm	~9%

heteroatoms and unsaturated bonds, and it decomposes at lower temperature with the formation of a carbon-based nanoparticle. The resultant FCN has high colloidal stability and stable fluorescence suitable for application as a cell-imaging probe.

EXPERIMENTAL SECTION

Materials. Thiamine hydrochloride (vitamin B_1), sodium tripolyphosphate ($Na_5P_3O_{10}$), sodium hexametaphosphate [$(NaPO_3)_n$], sodium phosphate monobasic (NaH_2PO_4), sodium phosphate dibasic (Na_2HPO_4), dialysis tube (benzoylated, MWCO ~ 2000 Da), Dulbecco's modified Eagle medium (DMEM), and methylthiazolyldiphenyltetrazolium bromide (MTT) were purchased from Sigma-Aldrich. HeLa and CHO cells were purchased from National Centre for Cell Science, Pune, India. Trisodium phosphate dodecahydrate ($Na_3PO_4{\cdot}12H_2O$) and ethylene glycol were bought from Merck.

Preparation of Blue- and Green-Emitting FCNs. A total of 1 g of thiamine hydrochloride was dissolved in 5 mL of ethylene glycol or water. Next, 0.1−10 g of phosphate salt was added to the solution and dissolved by sonnication. Next, the mixture was heated at ~90−130 °C for about 2 h. The solution color changed from colorless to deep brown. In some cases, the solution was dialyzed against water using a dialysis membrane. The resulting solution was used as a stock solution for various experiments.

QY Measurement. The QYs of the samples were measured using quinine sulfate as the reference (QY = 58% at 340 nm excitation).[29] The formula used for QY measurement is as follows:

$$(QY)_{Sm} = (QY)_{St}\frac{(PL\ area/OD)_{Sm}}{(PL\ area/OD)_{St}}\frac{\eta_{Sm}^{\ 2}}{\eta_{St}^{\ 2}}$$

where Sm indicates the sample, St indicates the standard, η is the refractive index of the solvent, "PL area" indicates the fluorescence area, and OD indicates the absorbance value.

In Vitro Cellular Labeling Experiments. HeLa and CHO cells were cultured in DMEM with 10% fetal bovine serum and 1% penicillin streptomycin with 5% CO_2 and at 37 °C temperature. In a chamber slide, the cells were cultured with 0.5 mL of media, mixed with 200 μL of a FCN solution, and incubated for 2 h. Then the incubation cells were washed with phosphate-buffered saline (PBS), fixed with 4% paraformaldehyde, mounted using 50% glycerol, and used for microscopic imaging.

Cytotoxicity Assay. Cytotoxicity measurement was performed using MTT-based assay. HeLa cells were incubated for 24 h with different doses of the FCN sample in 24-well plates. Next, cells were washed using a PBS solution. Then, 50 μL of a freshly prepared MTT solution (5 mg/mL) was mixed into each well and incubated for 4 h. After that, the violet formazan produced was dissolved in a 50% aqueous *N*,*N*-dimethylformamide (DMF) solution, and the absorbance was recorded at 570 nm using a microplate reader. The optical density was correlated with the cell viability, assuming 100% viability for the control sample without any FCN.

Instrumentation. Emission and excitation spectra were performed using a SynergyTM MX multimode microplate reader. Transmission electron microscopy (TEM) samples were prepared by putting a drop of a nanoparticle solution on a carbon-coated copper grid and observed with a FEI Tecnai G2 F20 microscope. X-ray photoelectron spectroscopy (XPS) was performed using an Omicron (series 0571) X-ray photoelectron spectrometer with a drop-cast nanoparticle solution. Time-correlation single-photon-counting (TCSPC) measurements were performed with Horiba Jobin Yvon IBH Fluorocube instruments after excitation with a 375 nm diode laser (IBHNanoLED). The fluorescence decay was obtained using a Hamamatsu MCP (R3809) photomultiplier tube and analyzed by *IBHDAS6* software. A total of 1 mL of a nanoparticle solution was diluted with distilled water and used for TCSPC measurement. Raman spectra with a 785 nm excitation laser were collected using an Agiltron R3000 Raman spectrometer. Fourier transform infrared (FTIR) spectroscopy was performed on a PerkinElmer Spectrum 100 FTIR spectrometer with solid KBr pellets. UV−visible absorption spectra were measured using a Shimadzu UV-2550 UV−visible spectrophotometer. The fluorescence images of the cell were captured by Carl Zeiss Apotome Imager Z1 and Olympus IX-81 fluorescence microscopes. Dynamic light scattering and ζ potential measurements were performed using a NanoZS (Malvern) instrument. Gel electrophoresis was carried out by a GE Healthcare miniVE vertical electrophoresis system.

dx.doi.org/10.1021/am500964d | ACS Appl. Mater. Interfaces 2014, 6, 7672−7679

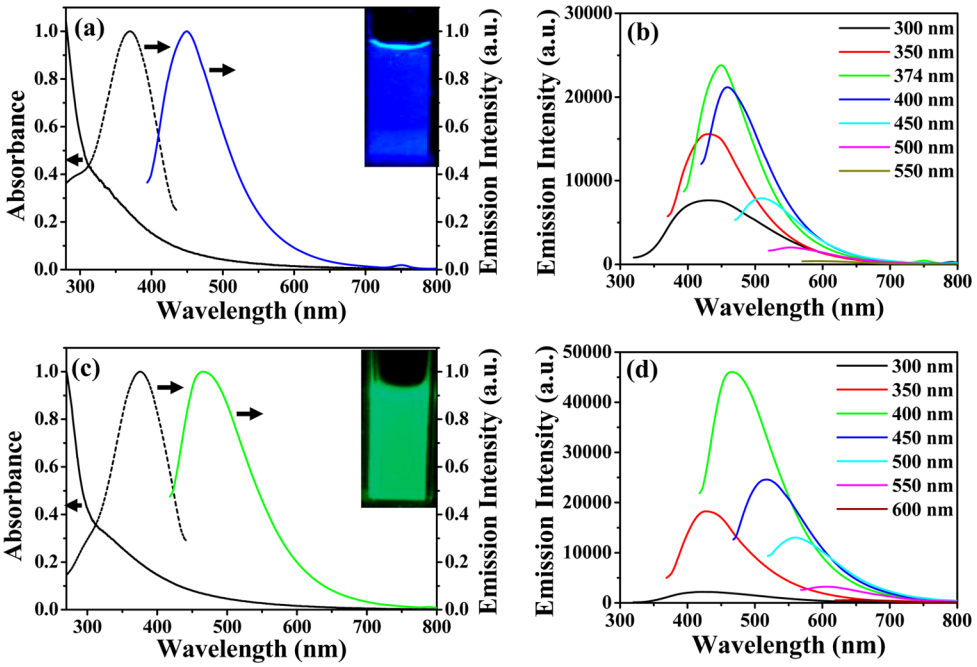

Figure 1. (a and b) Optical properties of blue-emitting FCN (FCN_{blue}) and (c and d) green-emitting FCN (FCN_{green}). Best fluorescence spectra (color line) of FCN_{blue} (a) and FCN_{green} (c) solutions with the corresponding absorption (solid line) and fluorescence excitation (dotted line) spectra. Inset: emission of the solution under a hand-held UV lamp. Emission spectra of FCN_{blue} (b) and FCN_{green} (d) at different excitation wavelengths.

RESULTS AND DISCUSSION

Synthesis Strategy. The synthesis approach of blue- and green-emitting FCNs is shown in Scheme 1. Thiamine hydrochloride and phosphate salt of different weight ratios are dissolved in ethylene glycol or water and heated at 90−130 °C for 2 h. Under these conditions, thiamine undergoes carbonization with the formation of FCN and phosphate can covalently attach on the growing FCN surface and/or adsorb as a capping ligand on the FCN surface. We have tested different reaction conditions in order to achieve FCN of high fluorescence QY and with different emission color [see Table 1 and Supporting Information (SI), Table S1]. We have tested different types of phosphates that include NaH_2PO_4, Na_2HPO_4, Na_3PO_4, H_3PO_4, sodium tripolyphosphate, and sodium hexametaphosphate. Water and ethylene glycol have been tested as solvents, and the reaction temperature has been varied between 90 and 130 °C. Ethylene glycol has been selected as the polar solvent particularly because of its high boiling point and good solubility of all reactants in this solvent. In some selected cases, syrupy phosphoric acid (H_3PO_4) has been tested as the solvent; however, product isolation becomes a difficult issue.

Results show that high-quality FCN can be synthesized with blue or green emission with fluorescence QYs between 5 and 76%. However, the quality and nature of FCN strongly depend on the carbonization condition. It is observed that the phosphate salts have a tremendous influence on the fluorescence QYs of FCN products. For example, FCN produced in the absence of any phosphate salt has a low fluorescence QY (<4%), but it increases up to 76% in the presence of phosphate salt. The quality of FCN also depends on the solvent, reaction temperature, and reaction time. Although an aqueous medium can produce blue-emitting FCNs, most of them are too small to observe under an electron microscope and pass through a dialysis membrane having MWCO ∼ 2000 Da. In contrast, FCNs produced in ethylene glycol under ∼130 °C are easily observable by TEM, although their fluorescence QY is lowered.

In general, blue-emitting FCNs are formed in most of the condition and they have higher fluorescence QYs than green-emitting FCNs. For example, blue-emitting FCNs can be synthesized by carbonization of aqueous thiamine at 90 °C in the presence of Na_2HPO_4, Na_3PO_4, H_3PO_4, sodium tripolyphosphate, and sodium hexametaphosphate. The FCNs produced under this condition have fluorescence QYs in the range of 25−76%. In contrast, green-emitting FCNs can be synthesized only under limited conditions. For example, green-emitting FCNs are formed upon heating an ethylene glycol solution of a mixture of thiamine and sodium tripolyphosphate at 130 °C. In addition, FCNs produced under this condition have fluorescence QYs in the range of 4−9%.

Characterization of FCNs. The optical properties of synthesized blue- and green-emitting FCNs are shown in Figure 1. The blue- and green-emitting FCNs are classified as FCN_{blue} and FCN_{green}, respectively. The solution of FCN_{blue} shows deep-blue emission and the solution of FCN_{green} shows green emission under conventional UV lamps. Each of the FCNs shows excitation-dependent emission spectra, and emission maxima red shifts with a red shifting of the excitation wavelength (Figure 1 and SI, Figures S1−S5). However, the most intense emission is observed at a certain excitation wavelength, and at either side of that wavelength, the emission intensity decreases. For example, the best excitation wavelength for FCN_{blue} is 375 nm, and the best excitation wavelength for FCN_{green} is 400 nm. Such types of excitation-dependent emission properties have also been observed earlier.[29,36,37] The sizes of FCN_{blue} and FCN_{green} have been examined under a TEM study. Although most of the aqueous-solvent-based FCN are TEM-invisible, FCNs synthesized in ethylene glycol are visible in TEM (Figure 2). The typical average size of FCN_{blue}

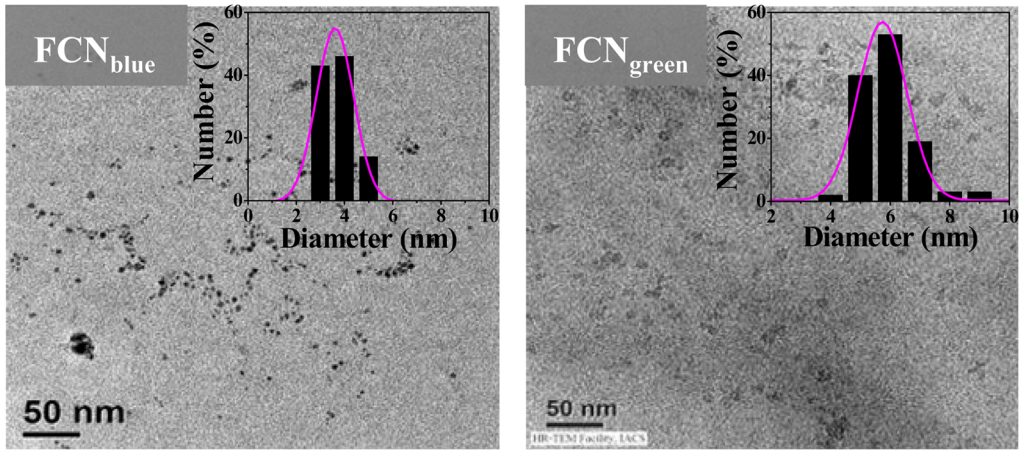

Figure 2. TEM images of FCN_{blue} and FCN_{green} with their corresponding size distribution histograms in the insets.

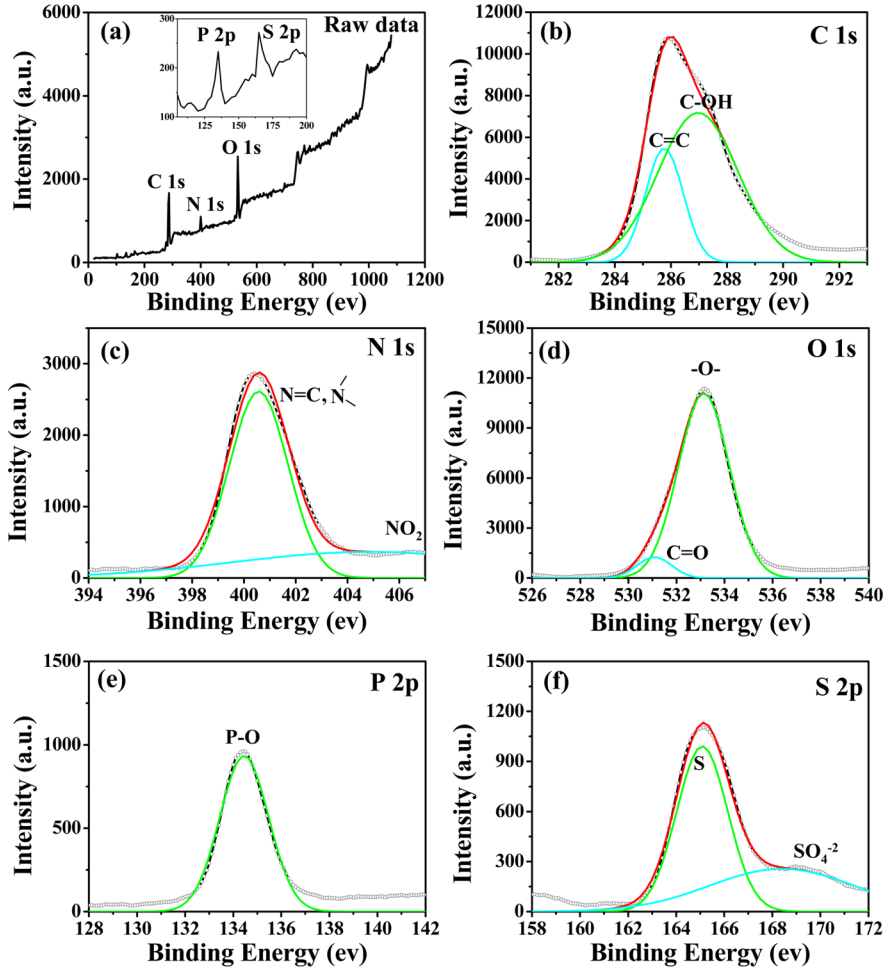

Figure 3. XPS spectra of FCN_{green} synthesized using sodium tripolyphosphate stabilizer. (a) Raw XPS data showing the presence of carbon, nitrogen, oxygen, sulfur, and phosphorus. (b) Deconvoluted C 1s spectrum with a peak at ~285 eV for sp^2 carbon atoms and a peak at ~287 eV for C−OH groups. (c) Deconvoluted N 1s spectrum with a peak at ~400.5 eV assigned for pyrrolic and pyridinic nitrogen in association with an oxygen functionality and a peak at 405 eV for NO_2 groups. (d) Deconvoluted O 1s spectrum with a peak at ~531 eV for C═O and a peak at ~533 eV for C−OH and/or C−O−C groups. (e) Deconvoluted P 2p spectrum at ~134.5eV for the P−O bond. (f) Deconvoluted S 2p spectrum with a peak at ~165 eV for elemental sulfur and a peak at 168.4 eV for oxidized sulfur.

is 3.7 ± 0.8 nm, and the average size of FCN_{green} is 5.9 ± 1.8 nm. The hydrodynamic sizes and surface charges of most of the FCNs are difficult to measure because of their small size. The relatively larger size FCNs prepared in ethylene glycol solvents can be measured. Results show that the hydrodynamic sizes of FCN_{blue} and FCN_{green} are 15 ± 2.5 and 28 ± 9.0 nm, respectively (SI, Figure S6). The polydispersity indexes measured for FCN_{blue} and FCN_{green} are 1.00 and 0.45, respectively. The surface charges of both of these nanoparticles are negative, as determined by their migration during

dx.doi.org/10.1021/am500964d | ACS Appl. Mater. Interfaces 2014, 6, 7672−7679

polyacrylamide-based gel electrophoresis (SI, Figure S7). The surface charges of both these nanoparticles are quantitatively determined, and the values are −4.3 and −2.0 mV for FCN_{blue} and FCN_{green}, respectively (SI, Figure S8).

The elemental composition has been determined from elemental analysis and XPS studies. Elemental analysis shows the presence of carbon, hydrogen, nitrogen, and sulfur in a weight ratio of 48:6:16:7, which is different from the elemental composition of thiamine, for which the weight ratio is 42:6:16:10. The XPS study also shows the presence of carbon as the major component along with other minor components like nitrogen, oxygen, sulfur, and phosphorus (Figure 3). The overall weight percent of elements present in FCN is C:H:N:O:S:P ∼ 45:6:14:27:5:3. The raw XPS data of FCN_{green} show signals corresponding to carbon, nitrogen, oxygen, sulfur, and phosphorus (Figure 3a). The C 1s XPS spectrum can be deconvoluted into two components (Figure 3b). Peaks at ∼285 and ∼287 eV can be attributed to carbon with C═C and C−OH groups, respectively.[29,36,38] In addition, the ratio of sp^2/sp^3 carbon is determined as ∼0.36. The deconvoluted N 1s spectrum shows a peak centered at ∼400.5 eV corresponding to pyrrolic and/or pyridinic nitrogen in association with an oxygen functionality[39,40] and a peak at ∼405 eV corresponding to NO_2 groups[41] (Figure 3c). The deconvoluted O 1s spectrum shows a peak at ∼531 eV corresponding to C═O and a peak at ∼533 eV corresponding to C−OH and/or C−O−C[42,43] (Figure 3d). Similarly, a deconvoluted P 2p spectrum shows a peak at ∼134.5 eV for P−O[29] (Figure 3e), and a deconvoluted S 2p spectrum shows a peak at ∼165 eV for elemental sulfur and a peak at 168.4 eV for oxidized sulfur[21] (Figure 3f).

Raman spectra of purified FCN shows prominent D and G bands at ∼1278 and ∼1638 cm^{-1}, respectively, with an I_D/I_G ratio of ∼1.33. This value is larger than that of graphene oxide and chemically reduced graphene, suggesting the presence of defects[29] (SI, Figure S9). The lifetime decay curve of FCN_{green} fits within three lifetime components ranging from the 0.4 to 5.0 ns time scale, indicating the presence of multiple radiative species[29] (SI, Figure S9).

The nature of the chemical bonding has also been estimated from a FTIR study (Figure 4 and SI, Figure S10). A FTIR study has been performed at different reaction times as well as for isolated and purified FCN samples. Results show that the signature of N−H deformation vibrations of vitamin B_1 at ∼700, ∼870, and ∼1530 cm^{-1} gradually disappears with time. In addition, the signature of the P−O−P bond of polyphosphate at ∼945 cm^{-1} decreases with time with the appearance of the Ar−O−P bond at ∼1210 cm^{-1}, demonstrating the attachment of phosphate to FCN.[44] Moreover, the original NH stretching band at ∼3490 cm^{-1} and the OH stretching band at ∼3420 cm^{-1} gradually merged into a broad band with the formation of FCN.

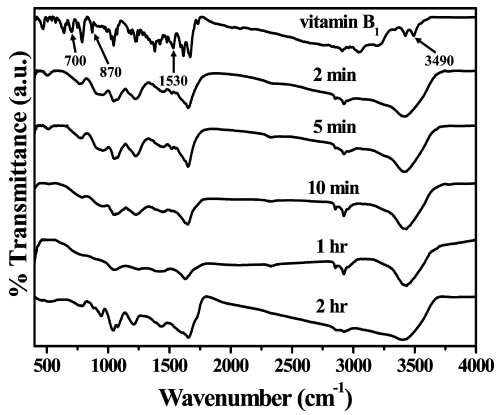

Figure 4. Time-dependent change of the FTIR spectrum of vitamin B_1 during the synthesis of FCN_{green}. Results show that the signature of N−H deformation vibrations of vitamin B_1 at ∼700, ∼870, and ∼1530 cm^{-1} gradually disappears with time. In addition, the original NH stretching band at ∼3490 cm^{-1} and the OH stretching band at ∼3420 cm^{-1} gradually merged into a broad band with the formation of FCN.

Origin of High Fluorescence. The origin of the fluorescence property of carbon nanoparticles is assumed because of the presence of isolated sp^2 carbon clusters and defect sites inside the carbon matrix.[1,29] The sp^2 carbon clusters with conjugated double bonds can strongly influence the band gap and optical property in the UV−visible region and hence can enhance the visible fluorescence. The higher ratio of sp^3 carbon atoms and heteroatoms like oxygen, nitrogen, sulfur, and phosphorus induces more defect sites in the sp^2 carbon clusters, giving rise to the enhanced fluorescence property.[1]

Considering all of these aspects, we presume that there are three distinct reasons for the enhanced fluorescence property of our FCN. First, the chemical structure of thiamine is unique because it contains several heteroatoms (four nitrogen, one sulfur, and one oxygen) along with five unsaturated double bonds (C═N and C═C) and carbonization occurs easily at relatively lower temperature. Thus, it is expected that heteroatoms are easily incorporated into the carbon nanoparticle matrix during the carbonization-based formation of FCN. In fact, elemental analysis shows a high percentage of heteroatoms in FCN. Thus, the structural feature of thiamine strongly influences the high fluorescence QY of FCN. Second, the carbonization condition is adjusted in such a way that it incorporates a significant percentage of phosphorus in the FCN matrix. Control experiments show that FCNs produced in the absence of any phosphate salt have very poor fluorescence. The incorporation of phosphorus in the FCN matrix is confirmed by FTIR based covalent attachment of phosphate with FCN. It is expected that the incorporation of phosphorus creates more defects in the sp^2 carbon clusters and induces fluorescence enhancement.[45] The other role of phosphate might be to restrict the particle size <6 nm via a capping action or covalent conjugation with growing FCN. Third, the carbonization temperature and time are adjusted in such a way that FCN attains optimum size (<6 nm) to achieve highest fluorescence. Control experiments show that if the carbonization temperature is >90 °C, then particle formation becomes insignificant even for >6 h of heating. Similarly, if the carbonization temperature is >130 °C, the fluorescence of FCN decreases with increased heating time. Thus, the particle size and emission color are controlled by varying the temperature in the range of 90−130 °C.

Application as a Bioimaging Probe. The application potential of FCNs as nontoxic cell-imaging probes has been investigated. The colloidal stability of as-synthesized FCN is tested under different aqueous buffer solutions and under physiological condition. Results show that the FCN solution remains stable for weeks and months (SI, Figure S11). In addition, the photostability of FCN has also been investigated by exposing the colloidal solution under UV irradiation. Results show that the FCN solution does not have a photobleaching problem and fluorescence remains intact even after 1 h of UV exposure (SI, Figure S12). Thus, consistent fluorescence under

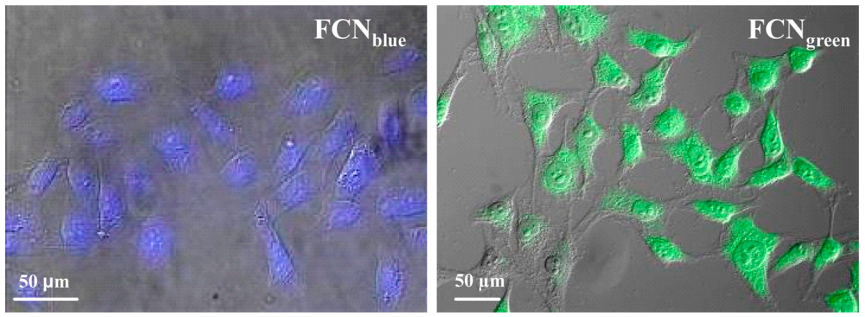

Figure 5. Fluorescence images of FCN-labeled cells. Live HeLa cells are incubated with FCN_{blue} (left panel) or FCN_{green} (right panel) for 2 h, and washed cells are imaged under a fluorescence microscope. Bright-field and fluorescence images are merged together for clarity.

a wide range of pH and under light exposure indicates that FCN can be useful as a stable biological imaging probe.

Application of FCN as a fluorescent cell label has been performed by incubating the FCN solution with different cell lines. Next, washed cells are fixed with 4% paraformaldehyde and imaged under a fluorescence microscope. Depending on the nature of FCN, different excitations are used to image the labeled cells. Results show that FCN acts as an excellent imaging probe and labels different cells (Figure 5 and SI, Figure S13). Usually, functionalization of a nanoparticle is essential for labeling of cells and cellular uptake of a nanoparticle occurs via receptor-mediated endocytosis.[29] In addition, charged nanoparticles and larger size particles enter into the cell via nonspecific uptake.[46] In contrast, presented FCN enters into the cell without any functionalization. Considering the fact that FCN has small size and a negative surface charge, nonspecific uptake of FCN should be insignificant. The tentative reason for labeling and uptake of FCN may be due to the vitamin B_1-like surface structure, which can induce transporter-mediated cell uptake, similar to cellular uptake of vitamin B_1.[47]

The cytotoxicity of our FCN has been investigated through conventional MTT assay (Figure 6). Results show that the cell viability is >95% at a concentration of 1 mg/mL. In contrast, it is known that CdSe-based QDs are cytotoxic in such a high dose.[48] The bioavailability and distribution of vitamins B_1 is well studied, and it is generally nontoxic in the cellular environment. It is a well-known fact that vitamin B_1 is an essential chemical for normal growth, and its deficiency causes various well-known diseases.[49−51] In particular, the nervous system is very sensitive to vitamin B_1 deficiency,[49−52] and vitamin B_1-dependent enzymes are present in all body cells.[52,53] Thus, it is expected that live cells should be able to tolerate a high concentration of vitamin B_1-derived FCN.

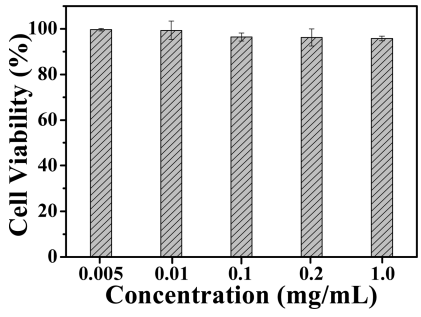

Figure 6. Results of a MTT-based cytotoxicity test of FCN_{green}, showing that they are nontoxic even at a substantially high dose. HeLa cells are incubated with different doses of FCN in a 24-well plate for 24 h. After the cells are washed, 50 μL of a freshly prepared MTT solution (5 mg/mL) is added to each well and incubated for 3−4 h. Next, the violet formazan complex formed is dissolved in a 50% aqueous DMF solution, and the absorbance is measured at 570 nm using a microplate reader. The optical density is correlated with the cell viability, assuming 100% viability for the control sample without any FCN.

CONCLUSION

In summary, vitamin B_1-derived blue- and green-emitting FCNs have been synthesized via a simple colloid−chemical carbonization approach. The high fluorescence originates from the chemical structure of vitamin B_1, which leads to the formation of a carbon nanoparticle with a significant percentage of nitrogen, sulfur, and other elements in their composition. This vitamin-derived nanoparticle shows insignificant cytotoxicity and can be used as a highly efficient fluorescent cell label.

ASSOCIATED CONTENT

Supporting Information

Optical property of FCN synthesized under different reaction conditions and other characterization details. This material is available free of charge via the Internet at http://pubs.acs.org.

AUTHOR INFORMATION

Corresponding Author

*. E-mail: camnrj@iacs.res.in. Telephone: +91-33-24734971. Fax: +91-33-24732805.

Notes

The authors declare no competing financial interest.

ACKNOWLEDGMENTS

This work is financially supported by DST and CSIR, Government of India. S.K.B. acknowledges CSIR India for a research fellowship. N.P. acknowledges IACS for a research fellowship. The authors are thankful for support from the XPS facility of DST Unit of Nanoscience, IACS.

REFERENCES

(1) Baker, S. N.; Baker, G. A. Luminescent Carbon Nanodots: Emergent Nanolights. *Angew. Chem., Int. Ed.* **2010**, *49*, 6726−6744.

(2) Cao, L.; Wang, X.; Meziani, M. J.; Lu, F. S.; Wang, H. F.; Luo, P. J. G.; Lin, Y.; Harruff, B. A.; Veca, L. M.; Murray, D.; Xie, S. Y.; Sun, Y. P. Carbon Dots for Multiphoton Bioimaging. *J. Am. Chem. Soc.* **2007**, *129*, 11318−11319.

(3) Yang, S. T.; Cao, L.; Luo, P. G. J.; Lu, F. S.; Wang, X.; Wang, H. F.; Meziani, M. J.; Liu, Y. F.; Qi, G.; Sun, Y. P. Carbon Dots for Optical Imaging in Vivo. *J. Am. Chem. Soc.* **2009**, *131*, 11308−11309.

(4) Michalet, X.; Pinaud, F. F.; Bentolila, L. A.; Tsay, J. M.; Doose, S.; Li, J. J.; Sundaresan, G.; Wu, A. M.; Gambhir, S. S.; Weiss, S. Quantum Dots for Live Cells, in Vivo Imaging, and Diagnostics. *Science* **2005**, *307*, 538−544.
(5) Peng, Z. A.; Peng, X. G. Formation of High-Quality CdTe, CdSe, and CdS Nanocrystals Using CdO as Precursor. *J. Am. Chem. Soc.* **2001**, *123*, 183−184.
(6) Medintz, I. L.; Uyeda, H. T.; Goldman, E. R.; Mattoussi, H. Quantum Dot Bioconjugates for Imaging, Labelling and Sensing. *Nat. Mater.* **2005**, *4*, 435−446.
(7) Pelley, J. L.; Daar, A. S.; Saner, M. A. State of Academic Knowledge on Toxicity and Biological Fate of Quantum Dots. *Toxicol. Sci.* **2009**, *112*, 276−296.
(8) Tasis, D.; Tagmatarchis, N.; Bianco, A.; Prato, M. Chemistry of Carbon Nanotubes. *Chem. Rev.* **2006**, *106*, 1105−1136.
(9) Diederich, F.; Thilgen, C. Covalent Fullerene Chemistry. *Science* **1996**, *271*, 317−323.
(10) Dreyer, D. R.; Park, S.; Bielawski, C. W.; Ruoff, R. S. The Chemistry of Graphene Oxide. *Chem. Soc. Rev.* **2010**, *39*, 228−240.
(11) Zhang, X. Q.; Zhang, X. Y.; Wang, S. Q.; Liu, M. Y.; Tao, L.; Wei, Y. Surfactant Modification of Aggregation-Induced Emission Material as Biocompatible Nanoparticles: Facile Preparation and Cell Imaging. *Nanoscale* **2013**, *5*, 147−150.
(12) Zhang, X. Q.; Liu, M. Y.; Yang, B.; Zhang, X. Y.; Chi, Z. G.; Liu, S. W.; Xu, J. R.; Wei, Y. Cross-Linkable Aggregation Induced Emission Dye Based Red Fluorescent Organic Nanoparticles and Their Cell Imaging Applications. *Polym. Chem.* **2013**, *4*, 5060−5064.
(13) Zhang, X. Q.; Liu, M. Y.; Yang, B.; Zhang, X. Y.; Wei, Y. Tetraphenylethene-Based Aggregation-Induced Emission Fluorescent Organic Nanoparticles: Facile Preparation and Cell Imaging Application. *Colloid Surf. B* **2013**, *112*, 81−86.
(14) Zhang, X. Q.; Zhang, X. Y.; Yang, B.; Hui, J. F.; Liu, M. Y.; Chi, Z. G.; Liu, S. W.; Xu, J. R.; Wei, Y. Facile Preparation and Cell Imaging Applications of Fluorescent Organic Nanoparticles that Combine AIE Dye and Ring-Opening Polymerization. *Polym. Chem.* **2014**, *5*, 318−322.
(15) Zhang, X. Q.; Zhang, X. Y.; Yang, B.; Hui, J. F.; Liu, M. Y.; Chi, Z. G.; Liu, S. W.; Xu, J. R.; Wei, Y. A Novel Method for Preparing AIE Dye Based Cross-Linked Fluorescent Polymeric Nanoparticles for Cell Imaging. *Polym. Chem.* **2014**, *5*, 683−688.
(16) Zhang, X. Q.; Zhang, X. Y.; Yang, B.; Hui, J. F.; Liu, M. Y.; Chi, Z. G.; Liu, S. W.; Xu, J. R.; Wei, Y. Novel Biocompatible Cross-Linked Fluorescent Polymeric Nanoparticles Based on an AIE Monomer. *J. Mater. Chem. C* **2014**, *2*, 816−820.
(17) Zhang, X. Y.; Zhang, X. Q.; Wang, S. Q.; Liu, M. Y.; Zhang, Y.; Tao, L.; Wei, Y. Facile Incorporation of Aggregation-Induced Emission Materials into Mesoporous Silica Nanoparticles for Intracellular Imaging and Cancer Therapy. *ACS Appl. Mater. Interfaces* **2013**, *5*, 1943−1947.
(18) Zhang, X. Y.; Zhang, X. Q.; Yang, B.; Liu, M. Y.; Liu, W. Y.; Chen, Y. W.; Wei, Y. Facile Fabrication and Cell Imaging Applications of Aggregation-Induced Emission Dye-Based Fluorescent Organic Nanoparticles. *Polym. Chem.* **2013**, *4*, 4317−4321.
(19) Zhang, X. Y.; Zhang, X. Q.; Yang, B.; Wang, S. Q.; Liu, M. Y.; Zhang, Y.; Tao, L.; Wei, Y. Aggregation-Induced Emission Material Based Fluorescent Organic Nanoparticles: Facile PEGylation and Cell Imaging Applications. *RSC Adv.* **2013**, *3*, 9633−9636.
(20) Das, P.; Saha, A.; Maity, A. R.; Ray, S. C.; Jana, N. R. Silicon Nanoparticle based Fuorescent Biological Label via Low Temperature Thermal Degradation of Chloroalkylsilane. *Nanoscale* **2013**, *5*, 5732−5737.
(21) Palmal, S.; Basiruddin, S. K.; Maity, A. R.; Ray, S. C.; Jana, N. R. Thiol-Directed Synthesis of Highly Fluorescent Gold Clusters and Their Conversion into Stable Imaging Nanoprobes. *Chem.—Eur. J.* **2013**, *19*, 943−949.
(22) Maity, A. R.; Palmal, S.; Basiruddin, S. K.; Karan, N. S.; Sarkar, S.; Pradhan, N.; Jana, N. R. Doped Semiconductor Nanocrystal based Fluorescent Cellular Imaging Probes. *Nanoscale* **2013**, *5*, 5506−5513.
(23) Li, H. T.; He, X. D.; Kang, Z. H.; Huang, H.; Liu, Y.; Liu, J. L.; Lian, S. Y.; Tsang, C. H. A.; Yang, X. B.; Lee, S. T. Water-Soluble Fluorescent Carbon Quantum Dots and Photocatalyst Design. *Angew. Chem., Int. Ed.* **2010**, *49*, 4430−4434.
(24) Suda, Y.; Ono, T.; Akazawa, M.; Sakai, Y.; Tsujino, J.; Homma, N. Preparation of Carbon Nanoparticles by Plasma-Assisted Pulsed Laser Deposition Method—Size and Binding Energy Dependence on Ambient Gas Pressure and Plasma Condition. *Thin Solid Films* **2002**, *415*, 15−20.
(25) Liu, H. P.; Ye, T.; Mao, C. D. Fluorescent Carbon Nanoparticles Derived from Candle Soot. *Angew. Chem., Int. Ed.* **2007**, *46*, 6473−6475.
(26) Fortunato, M. E.; Rostam-Abadi, M.; Suslick, K. S. Nanostructured Carbons Prepared by Ultrasonic Spray Pyrolysis. *Chem. Mater.* **2010**, *22*, 1610−1612.
(27) Yang, Z. C.; Wang, M.; Yong, A. M.; Wong, S. Y.; Zhang, X. H.; Tan, H.; Chang, A. Y.; Li, X.; Wang, J. Intrinsically Fluorescent Carbon Dots with Tunable Emission Derived from Hydrothermal Treatment of Glucose in the Presence of Monopotassium Phosphate. *Chem. Commun.* **2011**, *47*, 11615−11617.
(28) Zhu, H.; Wang, X. L.; Li, Y. L.; Wang, Z. J.; Yang, F.; Yang, X. R. Microwave Synthesis of Fluorescent Carbon Nanoparticles with Electrochemiluminescence Properties. *Chem. Commun.* **2009**, 5118−5120.
(29) Bhunia, S. K.; Saha, A.; Maity, A. R.; Ray, S. C.; Jana, N. R. Carbon Nanoparticle-Based Fluorescent Bioimaging Probes. *Sci. Rep.* **2013**, *3*, No. 1473.
(30) Pan, D. Y.; Zhang, J. C.; Li, Z.; Wu, C.; Yan, X. M.; Wu, M. H. Observation of pH-, Solvent-, Spin-, and Excitation-Dependent Blue Photoluminescence from Carbon Nanoparticles. *Chem. Commun.* **2010**, *46*, 3681−3683.
(31) Liu, R. L.; Wu, D. Q.; Liu, S. H.; Koynov, K.; Knoll, W.; Li, Q. An Aqueous Route to Multicolor Photoluminescent Carbon Dots Using Silica Spheres as Carriers. *Angew. Chem., Int. Ed.* **2009**, *48*, 4598−4601.
(32) Wang, X. H.; Qu, K. G.; Xu, B. L.; Ren, J. S.; Qu, X. G. Microwave Assisted One-Step Green Synthesis of Cell-Permeable Multicolor Photoluminescent Carbon Dots without Surface Passivation Reagents. *J. Mater. Chem.* **2011**, *21*, 2445−2450.
(33) Jiang, J.; He, Y.; Li, S. Y.; Cui, H. Amino Acids as the Source for Producing Carbon Nanodots: Microwave Assisted One-Step Synthesis, Intrinsic Photoluminescence Property and Intense Chemiluminescence Enhancement. *Chem. Commun.* **2012**, *48*, 9634−9636.
(34) Wei, W.; Xu, C.; Wu, L.; Wang, J.; Ren, J.; Qu, X. Non-Enzymatic-Browning-Reaction: A Versatile Route for Production of Nitrogen-Doped Carbon Dots with Tunable Multicolor Luminescent Display. *Sci. Rep.* **2014**, *4*, No. 3564.
(35) Yang, Z. C.; Li, X.; Wang, J. Intrinsically Fluorescent Nitrogen-Containing Carbon Nanoparticles Synthesized by a Hydrothermal Process. *Carbon* **2011**, *49*, 5207−5212.
(36) Sun, Y. P.; Zhou, B.; Lin, Y.; Wang, W.; Fernando, K. A. S.; Pathak, P.; Meziani, M. J.; Harruff, B. A.; Wang, X.; Wang, H. F.; Luo, P. J. G.; Yang, H.; Kose, M. E.; Chen, B. L.; Veca, L. M.; Xie, S. Y. Quantum-Sized Carbon Dots for Bright and Colorful Photoluminescence. *J. Am. Chem. Soc.* **2006**, *128*, 7756−7757.
(37) Ray, S. C.; Saha, A.; Jana, N. R.; Sarkar, R. Fluorescent Carbon Nanoparticles: Synthesis, Characterization, and Bioimaging Application. *J. Phys. Chem. C* **2009**, *113*, 18546−18551.
(38) Felten, A.; Bittencourt, C.; Pireaux, J. Gold Clusters on Oxygen Plasma Functionalized Carbon Nanotubes: XPS and TEM Studies. *J. Nanotechnol.* **2006**, *17*, 1954−1959.
(39) Choi, H. C.; Bae, S. Y.; Jang, W. S.; Park, J.; Song, H. J.; Shin, H. J.; Jung, H.; Ahn, J. P. Release of N_2 from the Carbon Nanotubes via High-Temperature Annealing. *J. Phys. Chem. B* **2005**, *109*, 1683−1688.
(40) Kapteijn, F.; Moulijn, J. A.; Matzner, S.; Boehm, H. P. The Development of Nitrogen Functionality in Model Chars During Gasification in CO_2 and O_2. *Carbon* **1999**, *37*, 1143−1150.
(41) Baltrusaitis, J.; Jayaweera, P. M.; Grassian, V. H. XPS Study of Nitrogen Dioxide Adsorption on Metal Oxide Particle Surfaces under

Different Environmental Conditions. *Phys. Chem. Chem. Phys.* **2009**, *11*, 8295−8305.
(42) Yue, Z. R.; Jiang, W.; Wang, L.; Gardner, S. D.; Pittman, C. U. Surface Characterization of Electrochemically Oxidized Carbon Fibers. *Carbon* **1999**, *37*, 1785−1796.
(43) Laszlo, K.; Tombacz, E.; Josepovits, K. Effect of Activation on the Surface Chemistry of Carbons from Polymer Precursors. *Carbon* **2001**, *39*, 1217−1228.
(44) Thomas, L. C.; Chittenden, A. Characteristic Infrared Absorption Frequencies of Organophosphorus Compounds—I. The phosphoryl (P═O) Group. *Spectrochim. Acta* **1964**, *20*, 467−487.
(45) Zhou, J.; Shan, X. Y.; Ma, J. J.; Gu, Y. M.; Qian, Z. S.; Chen, J. R.; Feng, H. Facile Synthesis of P-Doped Carbon Quantum Dots with Highly Efficient Photoluminescence. *RSC Adv.* **2014**, *4*, 5465−5468.
(46) Maity, A. R.; Jana, N. R. Chitosan-Cholesterol-Based Cellular Delivery of Anionic Nanoparticles. *J. Phys. Chem. C* **2011**, *115*, 137−144.
(47) Oyewumi, M. O.; Liu, S. Q.; Moscow, J. A.; Mumper, R. J. Specific Association of Thiamine-Coated Gadolinium Nanoparticles with Human Breast Cancer Cells Expressing Thiamine Transporters. *Bioconjugate Chem.* **2003**, *14*, 404−411.
(48) Derfus, A. M.; Chan, W. C. W.; Bhatia, S. N. Probing the Cytotoxicity of Semiconductor Quantum Dots. *Nano Lett.* **2004**, *4*, 11−18.
(49) Thornalley, P. J. The Potential Role of Thiamine (Vitamin B_1) in Diabetic Complications. *Curr. Diabetes Rev.* **2005**, *1*, 287−98.
(50) Meador, K.; Loring, D.; Nichols, M.; Zamrini, E.; Rivner, M.; Posas, H.; Thompson, E.; Moore, E. Preliminary Findings of High-Dose Thiamine in Dementia of Alzheimer's Type. *J. Geriatr. Psych. Neurol.* **1993**, *6*, 222−9.
(51) Mimori, Y.; Katsuoka, H.; Nakamura, S. Thiamine Therapy in Alzheimer's Disease. *Metab. Brain Dis.* **1996**, *11*, 89−94.
(52) Shils, M. E.; Shike, M.; Ross, A. C.; Caballero, B.; Cousins, R. J. *Modern Nutrition in Health and Disease*; Lippincott Williams & Wilkins: Baltimore, MD, 2006.
(53) Stanbury, J. B.; Wyngaarden, J. B.; Fredrickson, D. S. Goldstein, J. L.; Brown, M. S. *The Metabolic Basis of Inherited Disease*; McGraw-Hill: New York, 1983.